

Thermal cycle fatigue behavior on the dissimilar material joint

Y. Fukuzawa, S. Nagasawa, H. Takahashi and S. Hikotani

Department of Mechanical Engineering, Nagaoka University of Technology,
Kamitomioka, Nagaoka, 940-2188, Japan

Abstract

As many types of dissimilar material joint are fabricated in high temperature atmosphere, the tensile residual stress occurs around the interface during cooling procedure due to the difference of mechanical and physical properties between dissimilar materials. Various researches have been performed in order to relax the tensile residual stress and enhance the bonding strength on the bonded dissimilar materials. The interface shape is one of the most effective factor to obtain the high bonding strength. On the other hand, the interface strength decreases under the thermal cycle fatigue condition, due to the increasing of the residual stress for every thermal cycle. In this study, to obtain the long thermal fatigue life the interface shape effects on the bonding strength under thermal cycle fatigue condition was researched. Ceramics-metal joints that were machined to the proper interface shape by Electrical Discharge Machining Method were fabricated. The variations of bonding strength were estimated on the thermal cycle test practically. Also the analysis of the residual stress value and distribution around the interface was carried out with FEM. Comparing with results of the experimental and numerical analysis, suitable interface shape for dissimilar material joint under thermal cycle condition was discussed.

Keywords: Dissimilar joint, Interface shape, Interface strength, residual stress, thermal cycle fatigue, Electrical discharge machining

1. Introduction

When the ceramics-metal joint is fabricated by the diffusion bonding method at high temperature, the tensile residual stress is generated during the cooling process at the bonding interface, due to the difference of mechanical properties between dissimilar materials such as thermal expansion coefficients and Young's modulus. It reduces the bonding strength to the below of the interface strength. Therefore, it is important to estimate the residual thermal stress value and its distribution by experimental and analytical method. The effects of interface shape for the bonding strength have been reported by FEM analysis and practical tensile tests^[1-3]. Though joint was cooled under inhomogeneous temperature field in practice, many studies of the FEM analysis have been carried out in the uniform cooling conditions. On the inhomogeneous temperature it was assumed that the heat transfer occurred from exterior and osculating plane to inside of joint body. So sometime the experimental data did not coincide with the FEM analysis. It was also considered that the residual stress generation process would be much change on the

thermal cycle tests.

In this study, to clarify the effect of thermal cycle fatigue behavior on the bonding strength considering the interface shapes, FEM analysis and tensile tests were carried out.

2. Experimental

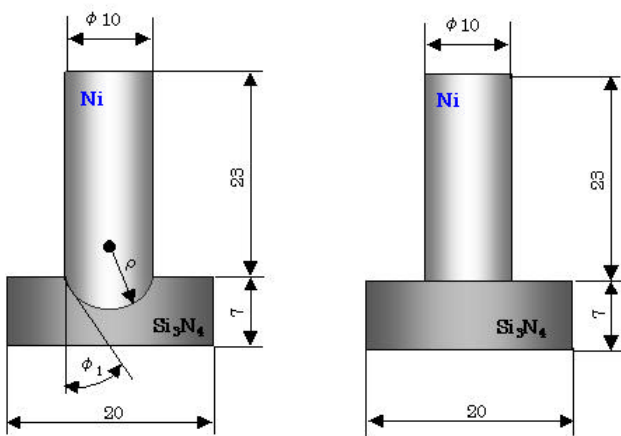
2-1 Specification of experiment

Sintered Si_3N_4 (ceramics) which is square plate (the side length: $2R_1=20[\text{mm}]$ and, thickness: $Z_1= 7[\text{mm}]$) and commercial pure Ni (metal) which is a cylindrical bar (Diameter: $2R_2=10[\text{mm}]$, height: $Z_2= 23[\text{mm}]$) are bonded by diffusion method with Ag (69wt%)-Cu (7.25wt%)-In (12.5wt%)-Ti (1.25wt%) solder in the vacuum furnace. The initial thickness of brazing metal is 0.2[mm]. The bonding conditions are described in Table 1.

Table 1 Joint processing condition

Atmosphere / Torr	Vacuum ($<10^{-6}$)
Joining temperature / K	1123
Joining pressure / MPa	2
Pressing time / sec	600
Furnace heating / K sec^{-1}	0.144
Furnace cooling / K sec^{-1}	-0.1 (1123[K] 723[K]) -0.03 (723[K] 293[K]) [-0.077 (1123[K] 293[K])]

The designed profile of joint is shown in Fig.1. Various spherical interfaces were machined for the joints. The insulating ceramics of Si_3N_4 were machined by the electrical discharge machining (EDM) method, which was proposed and named “assisting electrode method” by authors^[4] as shown in Fig.2. The Ni cylinder was machined by lathe machining and used for the electrode of EDM. The joint angle ϕ was defined as a geometrical angle between the tangential line at the interface edge and the outer surface of metal side. The joint angles ϕ_1 were chosen 33.6,51.2,60,71.8,90 [deg]. The bonding strength of each shapes were evaluated by the tensile test for the jointed material and after thermal cycle treatment at room temperature. The thermal cycle tests were carried out on the following conditions as shown in Fig. 3 and Table 2. The fracture surface profiles were observed by SEM and the fracture angles were measured by optical Microscope .



(a) Concave $\phi_1 = 90.0[\text{deg.}]$ (b) Flat $\phi_1 = 90.0[\text{deg.}]$

Fig.1 Experimental Si_3N_4 -Ni joint model

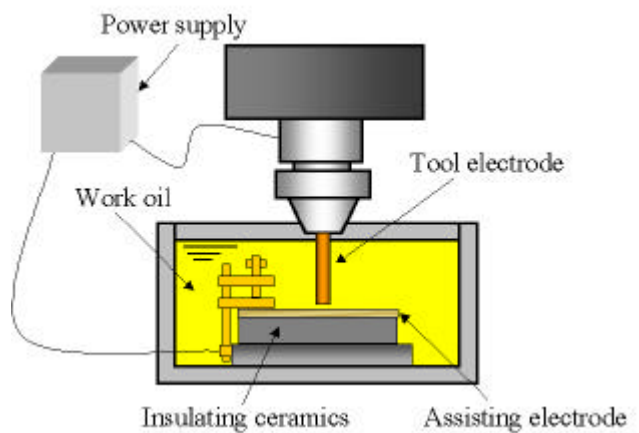


Fig.2 Schematic illustration of EDM method for insulating ceramics

Table 2 Thermal cycle conditions

Thermal cycle temperature / K	473,573,673
Atmosphere	Air
Inside furnace keep time / sec	300
Out of furnace keep time / sec	600
Thermal cycle number / cycle	1,5
Heating speed (293 573K)/K sec ⁻¹	3.78
Cooling speed (573 293K)/K sec ⁻¹	0.67

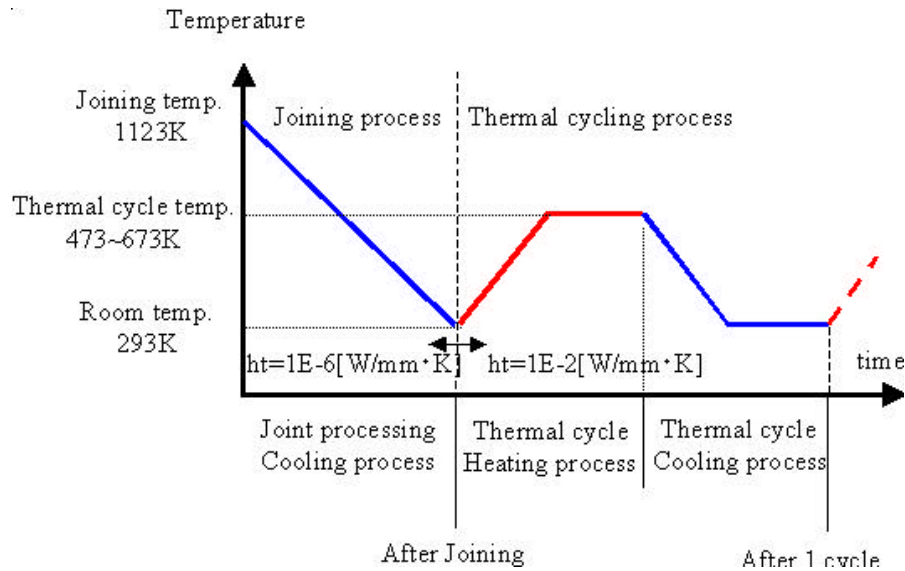


Fig.3 Thermal cycle fatigue diagram

2-2 Numerical analysis model

$\text{Si}_3\text{N}_4\text{-Ni}$ joint model, which had various spherical shapes, was chosen for FEM analysis. The axisymmetric bonded half of two dissimilar materials were considered with the cylindrical coordinates (z,r). The joint angles ϕ were selected the same shapes of experimental specimens. A quadrilateral axisymmetric ring element was used in this model, and mesh size of element was highly refined at the edge of interface (number of all elements 2304, the minimum subdivided ratio $r/R=z/Z=0.001$, subdivided ratio of two neighborhood elements: 0.7 as shown in Fig.4. The analysis was carried out on based on following assumptions. (1) Joining process of two isotropic materials was carried out perfectly at the bonding temperature 1123K. (2) The cooling process was carried out from the bonding to the room temperature under the inhomogeneous conditions. (3) Si_3N_4 was regarded as an elastic body. Ni was regarded as an elasto-plastic body. (4) All the displacement was geometrically considered as large and the strain was considered as finite strain.

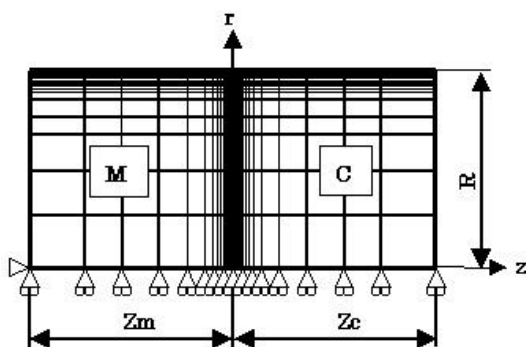


Fig. 4 Subdivided element model of bonded structure ($\phi_1=\phi_2=90.0[\text{deg.}]$)

Table 3 Mechanical properties of used materials

	Si_3N_4	Ni
Conductivity / $\text{J mm}^{-1} \text{sec}^{-1} \text{K}^{-1}$	0.029	0.088-0.0595
Density / 10^{-6}kg mm^3	3.20	8.90
Specific heat / $\text{J kg}^{-1} \text{K}^{-1}$	711.28	435.0-578.0
Young's modulus / GPa	274.59	206.0-107.0
Poisson's ratio / -	0.27	0.30
Thermal expansion / 10^{-6}K^{-1}	3.5	13.4-20.0
Yield strength / MPa	-	539.0-38.0
Coefficient of work-hardening / MPa	-	617.0-0.38

The mechanical properties of Ni depend on temperature. The mechanical properties of Si_3N_4 and Ni that were used for this analysis were shown in Table 3. The major discussion has been focused here on the σ_{zz} stress on the ceramics outer surface and interface.

3. Results and Discussions

Fig.5 shows experimental results of tensile strength for after joining treatment on each interface angle θ_1 . The maximum bonding strength identified at near the interface angle of 51.8 [deg]. It indicated that the bonding strength depended to the interface angle. Fig.6 shows the typical fracture patterns of joint. The fracture occurred at the bonding interface and internal ceramic side except the interface angle 51.3[deg]. On the 51.3 [deg] the failure propagated to the direction of outer surface of ceramics. It had small interface area. The relation between the fracture and interface angles was shown in Fig.7. The bonding strength increased with decreasing the fracture angle except the angle of 33.8[deg]. It indicated that the bonding strength depended on the crack propagation direction. When the fracture occurred near the outer surface of ceramics, the maximum bonding strength was obtained. Fig.8 shows the relationship between the interface angle and bonding strength on each thermal cycle temperature and cycle numbers. The same relations between bonding strength and interface angle were obtained, but the bonding strength values decreased with increasing the thermal cycle temperature and cycle numbers. The fracture angles of the thermal cycle tests changed comparison with the “after joining body” as shown in Fig.9. On the thermal cycle tests, the fracture propagation angle of outer interface circle became flatter than the “after joining” and turned to spherical shapes at the inside of interface position. In order to compare with the results of bonding strength after thermal cycle treatment and FEM analysis, the distribution of σ_{zz} stresses on the interface ceramics surface was calculated. The results are shown in Fig.10 (a), “after joining”, and (b) which is cycle temperature of 673 K and 5 cycles.

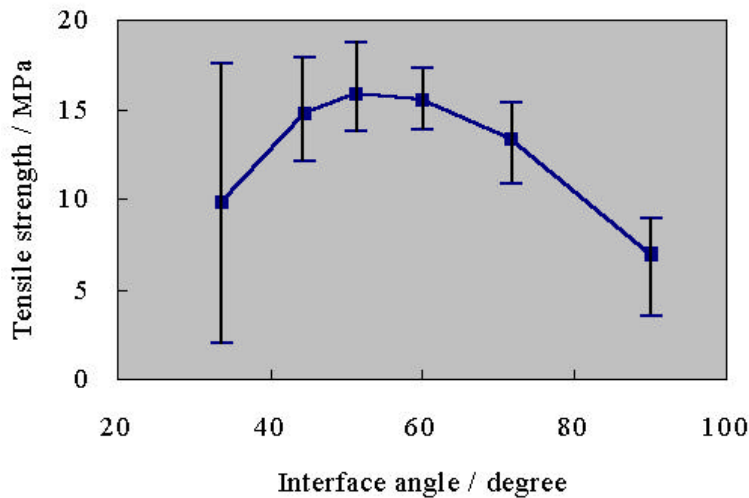


Fig. 5 Relation between interface and tensile strength

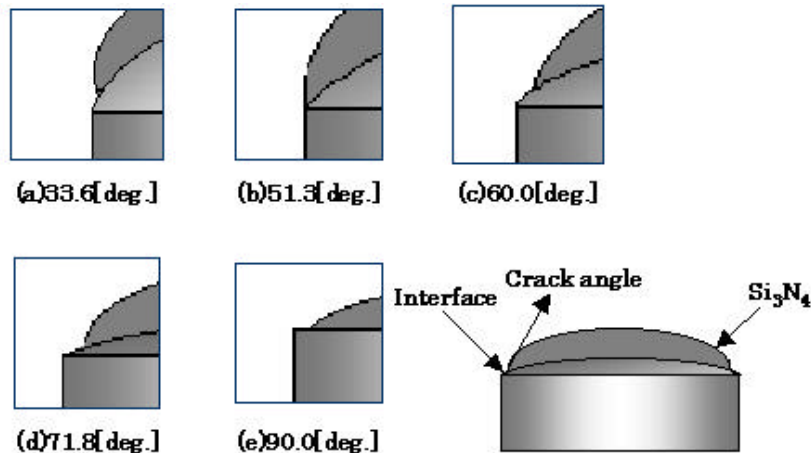


Fig.6 Schematic illustration of fracture surface models

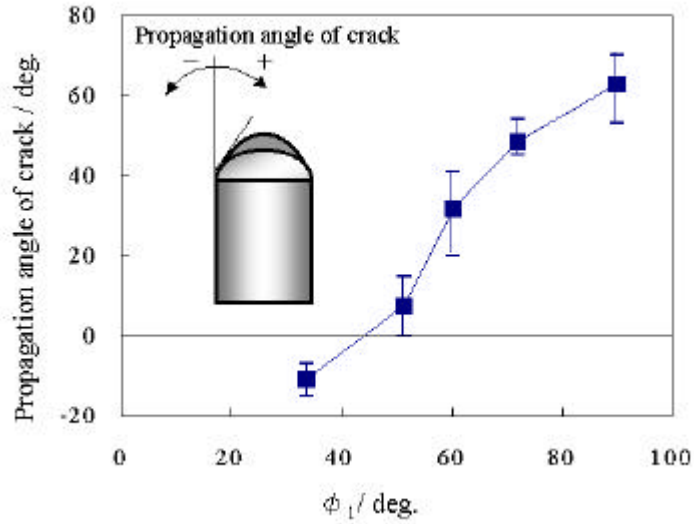


Fig.7 Relation between joint angle ϕ_1 and propagation angle of crack

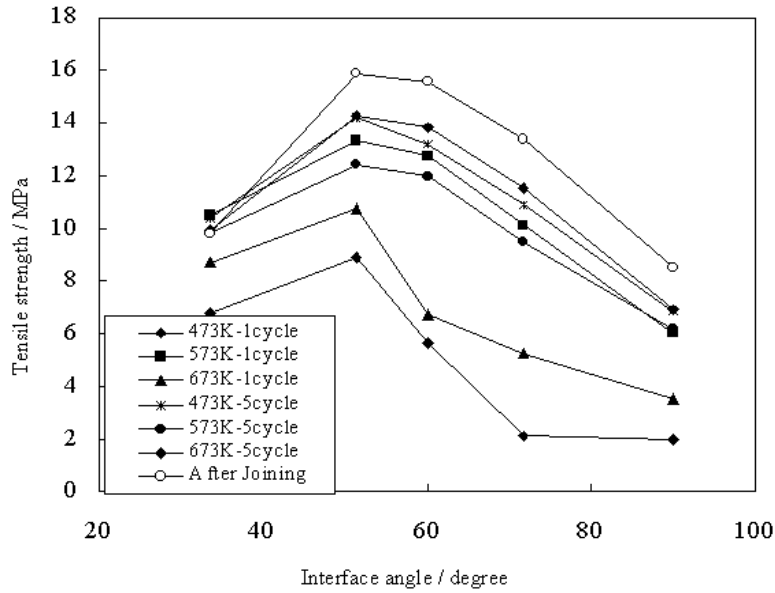


Fig.8 Relation between Interface angle and tensile strength

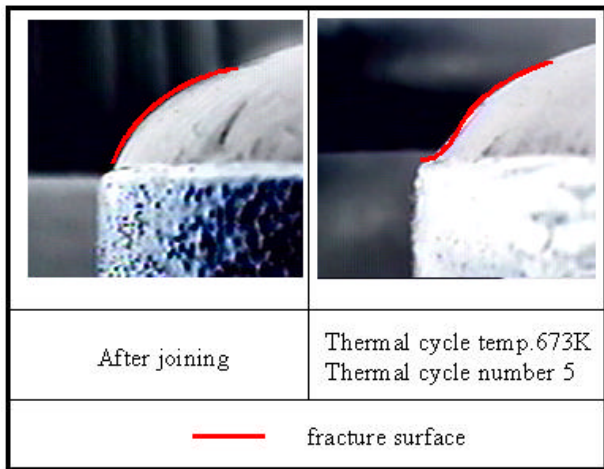


Fig.9 Fracture surface

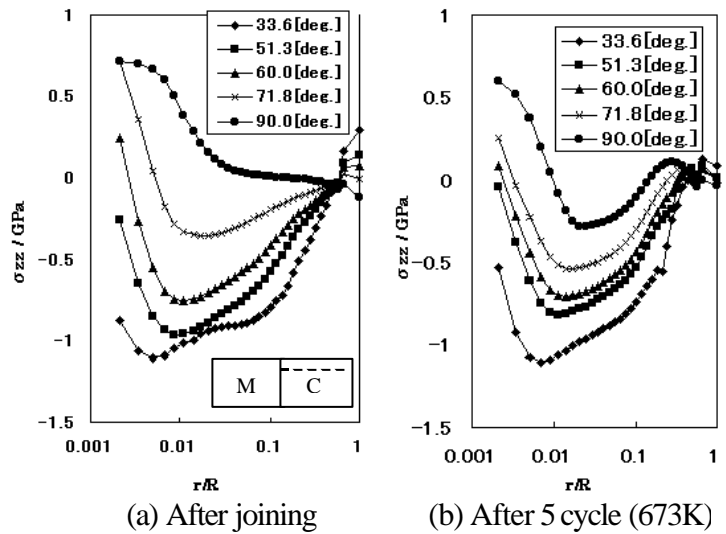


Fig.10 Effect of thermal cycle temperature of σ_{zz} of ceramics side interface

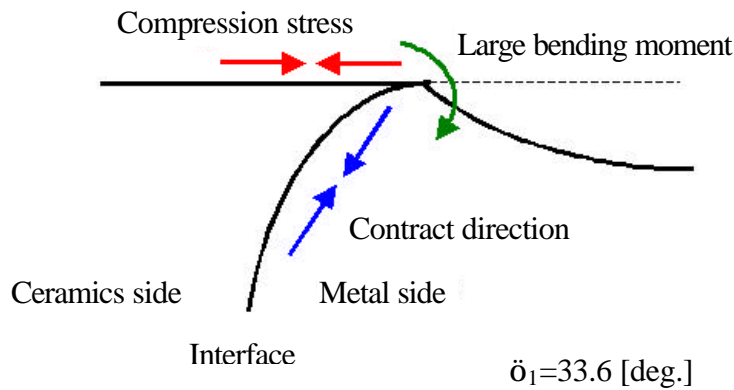


Fig.11 Mechanism of bending by metal contract

As reported before^[5], the residual thermal stress values and distribution were varied with the cooling rate and volume of body that was evaluated from the heat transfer coefficient (ht), on the numerical analysis and joint volume. On the joint volume of this experiment, the uniformly cooling condition (furnace cool on the bonding treatment) was accomplished at the heat transfer coefficient value, $ht = 10^{-6} [W \text{ mm}^2 \text{ K}^{-1}]$, and $ht = 10^{-2} [W \text{ mm}^2 \text{ K}^{-1}]$ corresponded to the cooling rate of thermal cycle test in which was inhomogeneous cooling condition. On the above FEM analysis the calculations were carried out with the above ht values for the bonding and thermal cycle treatments. The σ_{zz} distributed from the tensile to compressive region. When the tensile stress was applied, the distribution of σ_{zz} moved to tensile side^[6]. In the $\sigma_{zz} - r/R$ curve below $0.1r/R$, the position of minimum σ_{zz} moved to compression side with reducing the interface angle and to the interface surface. The values increased with increasing the cycle temperature and numbers. The inclination of $\sigma_{zz} - r/R$ curve near the interface became large, it corresponded to the reducing bonding strength on the thermal cycle rests. The variations of fractured angle around the outer interface were also explained by the inclination. On the interface angle of $33.6[\text{deg}]$, the bending moment must be considered as shown in Fig.11. So the bonding strength decreased than the $51.8[\text{deg}]$ case.

4. Conclusions

The influence of interface angle for the bonding strength was investigated on the thermal cycle conditions by experimental test and FEM analysis. The following conclusions were obtained.

- (1) The relations between the bonding strength and interface shape angle on the thermal cycle fatigue were similar to the after joining. The suitable interface angle for joining was detected on the thermal cycle test also. The bonding strengths decreased with increasing the cycle temperature and numbers.
- (2) The fractured angles depended on the interface angle and the thermal cycle conditions.
- (3) The fracture behaviors were explained with the FEM analysis, in which the inhomogeneous cooling process was considered.

References

1. S.Nagasawa, Y.Fukuzawa, Y.Yokoyama and M.Tateno, (2000) Adv. In Computational Eng.&Sci. Tech.Sci. Press, pp.1026-1030.
2. M.Tateno, Y.Fukuzawa, S.Nagasawa, H.Sakuta and Y.Kojima, (1993) Trans. Mat. Res. Soc.Jpn. Vol. 16B, pp.1101-1104.
3. Y.Fukuzawa, Y.Kojima, M.Tateno and N.Mohri, (1993) Trans. Mat. Res. Soc.Jpn. Vol. 16B, pp.1097-1100.
4. Y.Fukuzawa, N.Mohri and T.Tani, (1997) Int.J.of Electrical Machining, 2, pp.25-30.
5. S.Nagasawa, Y.Fukuzawa, H.Takahashi, T.Yamada, H.Sakuta and M.Tateno, (1997) Joining ceramics, Glass and Metal DVS, 120-123.
6. Y.Fukuzawa, S.Nagasawa, H.Takahashi, H.Sakuta, M.Tateno and Y.Kuboyama, (1996) Interface Science and Materials Interconnection Proc.of JIMIS-8 pp.463-466.